Electronic Supplementary Information

Multi-stimuli-responsive nanomicelles fabricated using synthetic polymer polylysine conjugates for tumor microenvironment dependent drug delivery

Rimesh Augustine,[a] Dae-Kyoung Kim,[b] Nagendra Kalva,[a] Kuen Hee Eom,[a] Jae Ho Kim,[*,b] Il Kim[*,a]

[a] BK21 PLUS Center for Advanced Chemical Technology, Dept. of Chemical engineering & Polymer Science and Engineering, Pusan National University, Busan 46241, Republic of Korea.

[b] Department of Physiology, School of Medicine, Pusan National University, Yangsan 626-870, Gyeongsangnam-do, Republic of Korea.

Contents

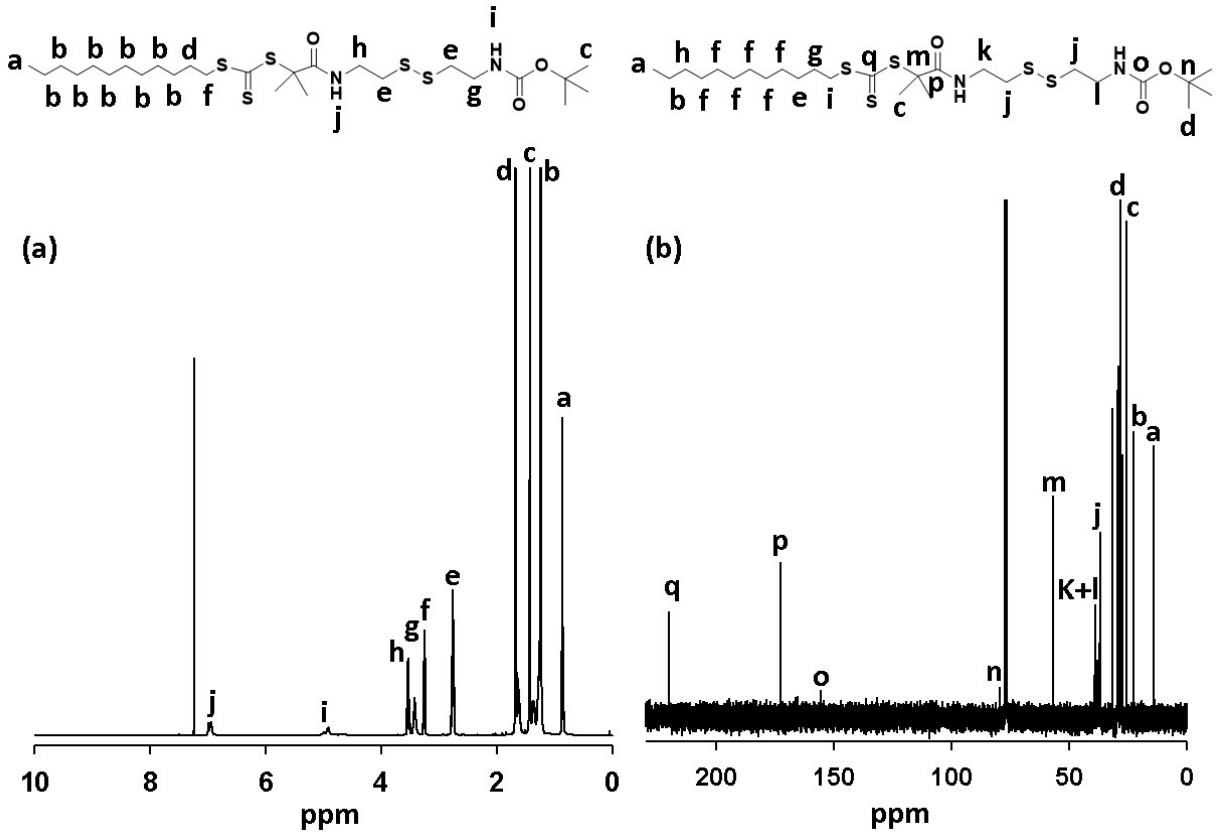

Fig. S1. (a) ^{1}H and (b) ^{13}C NMR spectra of the RAFT CTA-2.

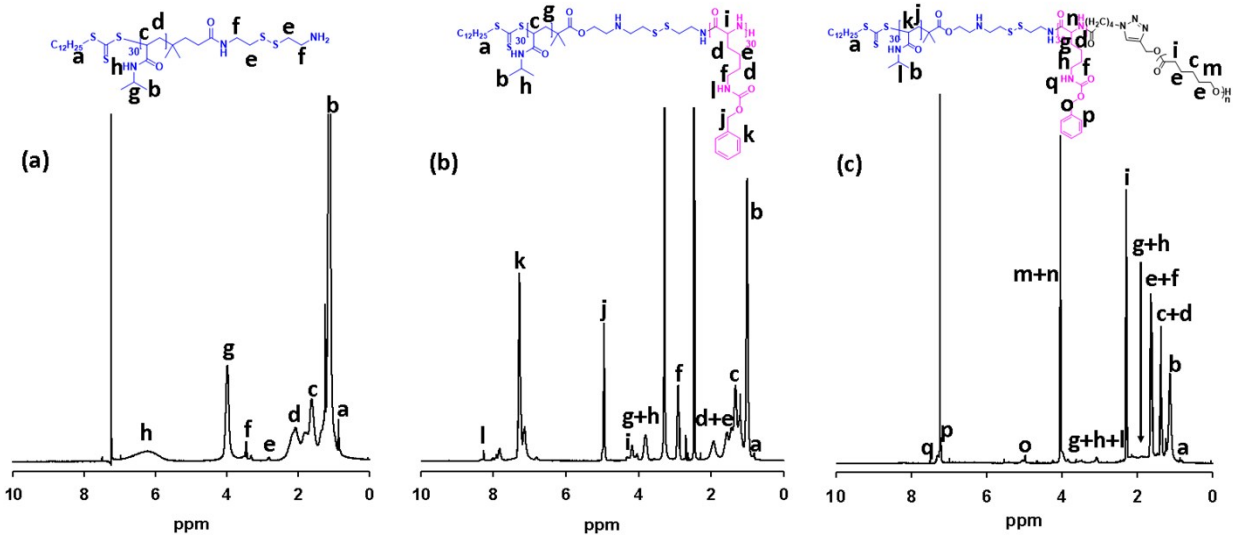

Fig. S2. ^{1}H NMR spectra of the (a) p(NIPAM)-NH_2, (b) p(NIPAM)$_{30}$-SS-*b*-p(Lys)$_{30}$ and (c) p(NIPAM)$_{30}$-SS-*b*-p(Lys)$_{30}$-*b*-p(CL)$_{125}$.

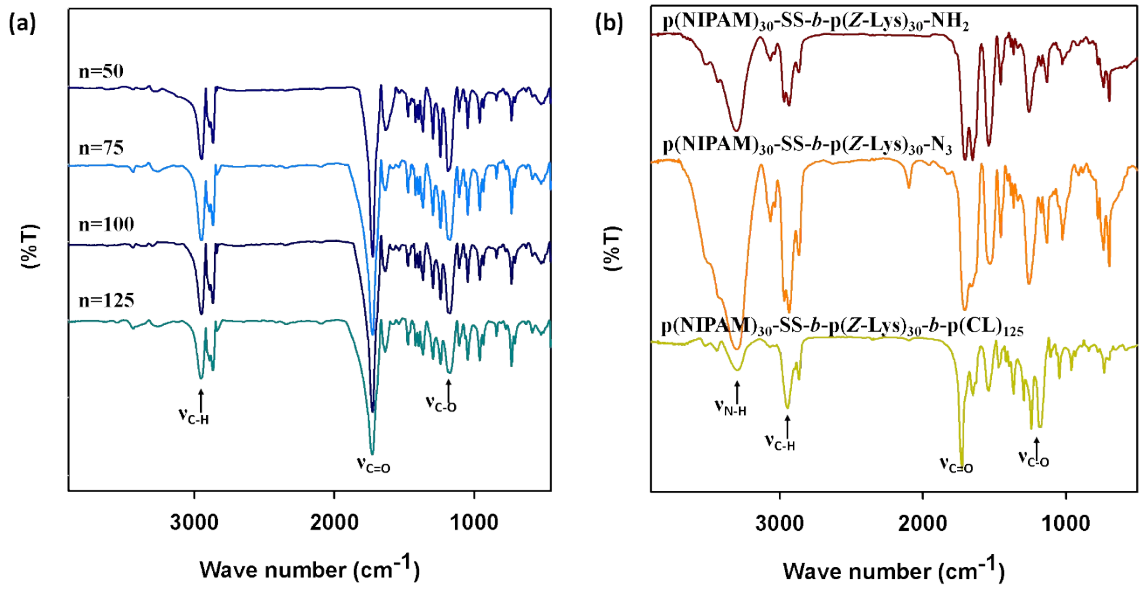

Fig. S3. FTIR profiles of (a) alkyne terminated polycaprolactone and (b) $p(NIPAM)_{30}$-SS-*b*-$p(Lys)_{30}$-*b*-$p(CL)_{125}$.

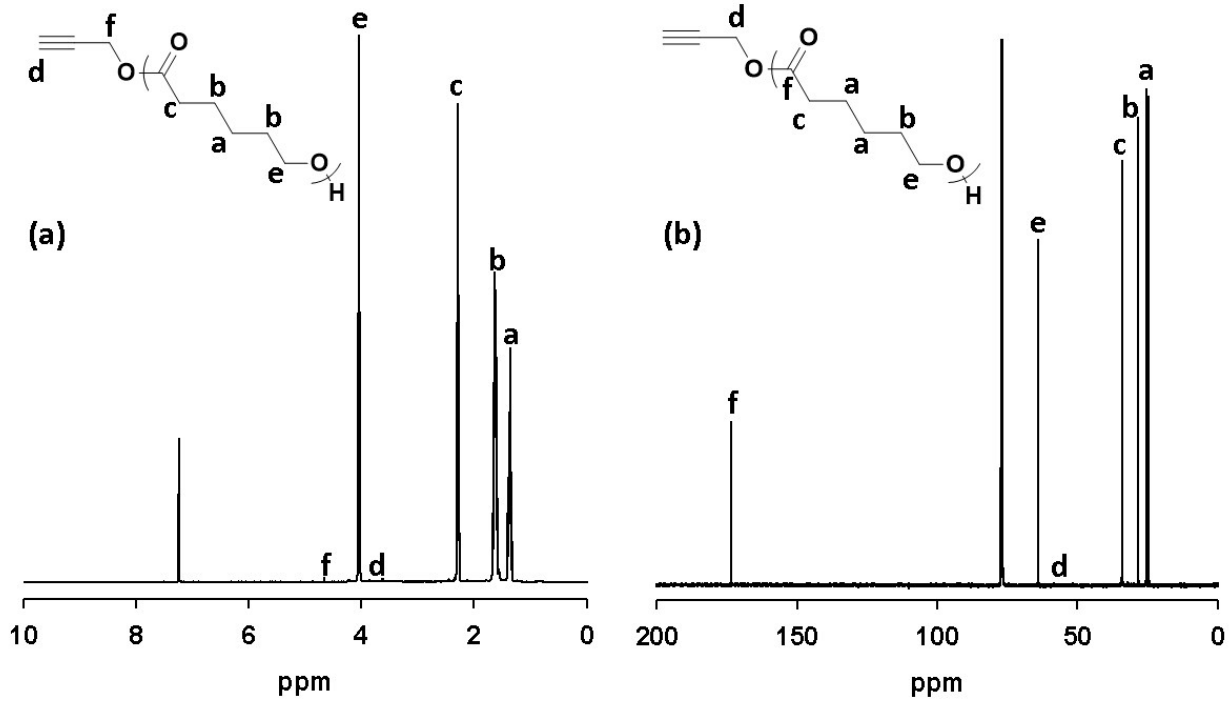

Fig. S4. (a) ^{1}H and (b) ^{13}C NMR spectra of the alkyne terminated polycaprolactone.

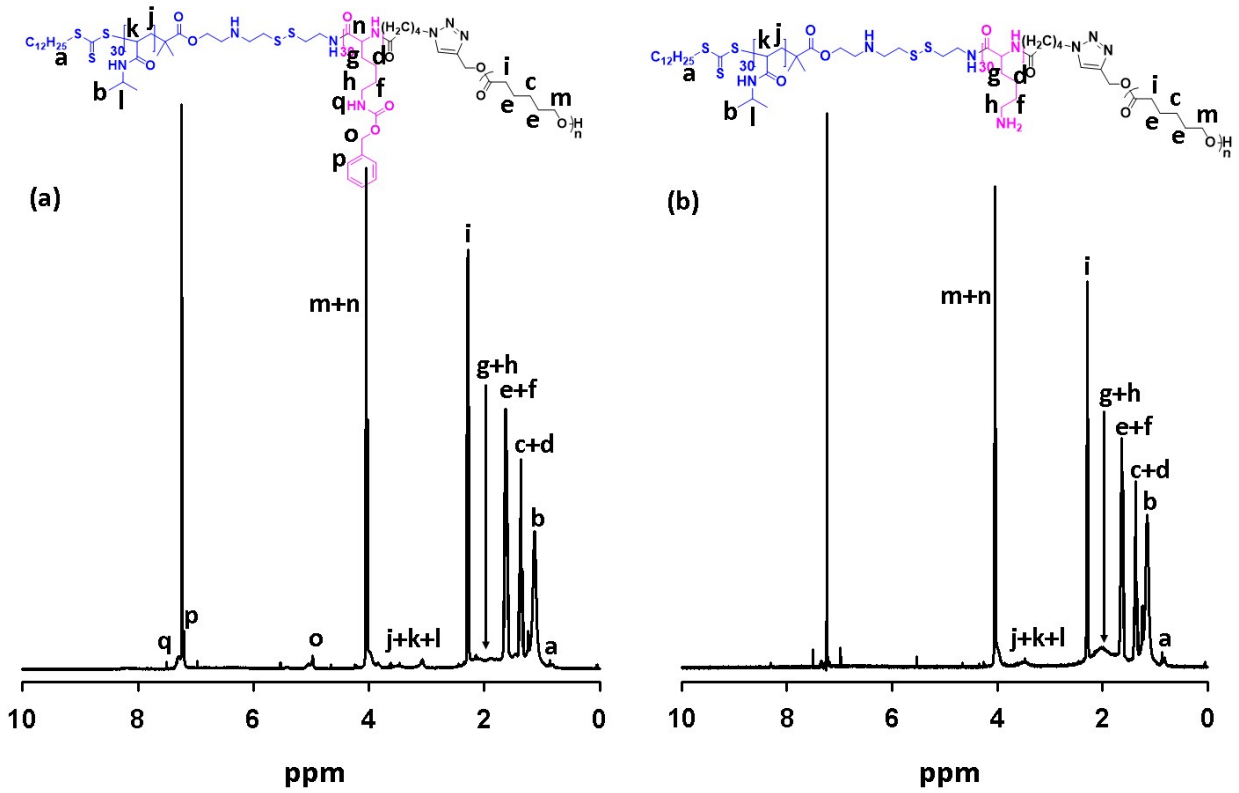

Fig. S5. ^{1}H NMR spectra of (a) protected and (b) deprotected p(NIPAM)$_{30}$-SS-*b*-p(Lys)$_{30}$-*b*-p(CL)$_{125}$.

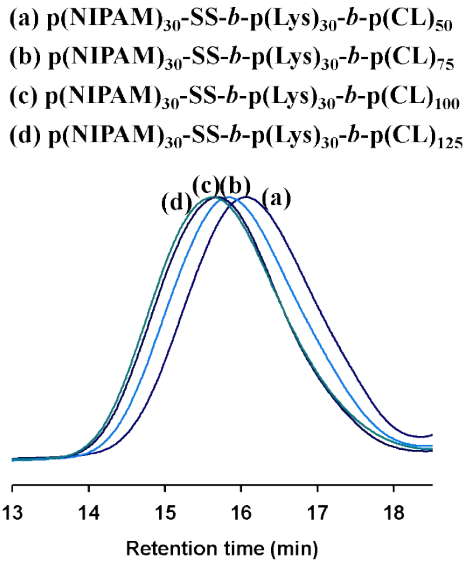

Fig. S6. (i) GPC curves of p(NIPAM)$_{30}$-*b*-p(Lys)$_{30}$-*b*-p(CL)$_{n}$.

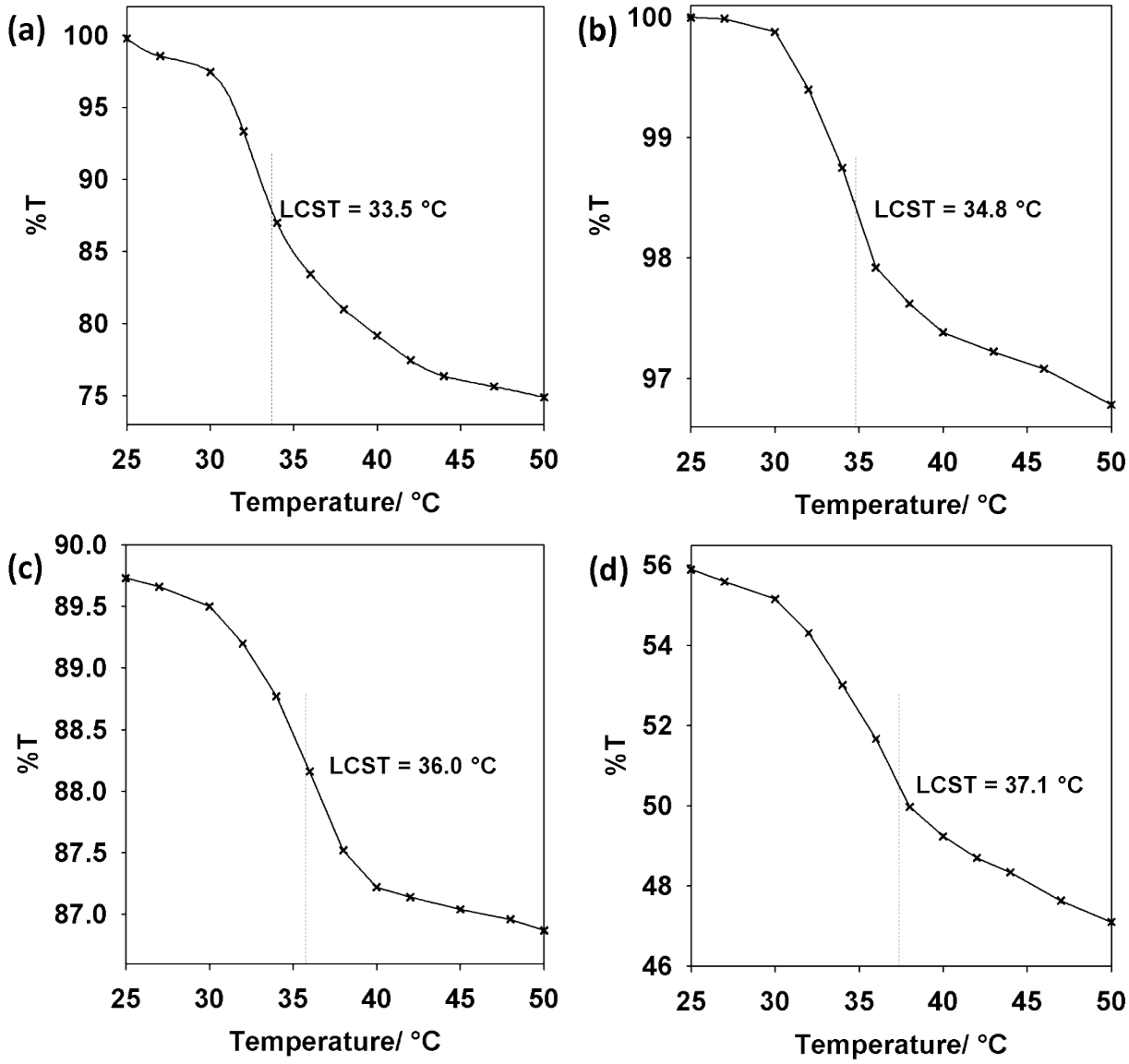

Fig. S7. Transmittance verses temperature curves for aqueous solution of (a) p(NIPAM)$_{30}$-SS-*b*-p(Lys)$_{30}$-*b*-p(CL)$_{50}$, (b) p(NIPAM)$_{30}$-SS-*b*-p(Lys)$_{30}$-*b*-p(CL)$_{75}$, (c) p(NIPAM)$_{30}$-SS-*b*-p(Lys)$_{30}$-*b*-p(CL)$_{100}$ and (d) p(NIPAM)$_{30}$-SS-*b*-p(Lys)$_{30}$-*b*-p(CL)$_{125}$ at pH 7.4.

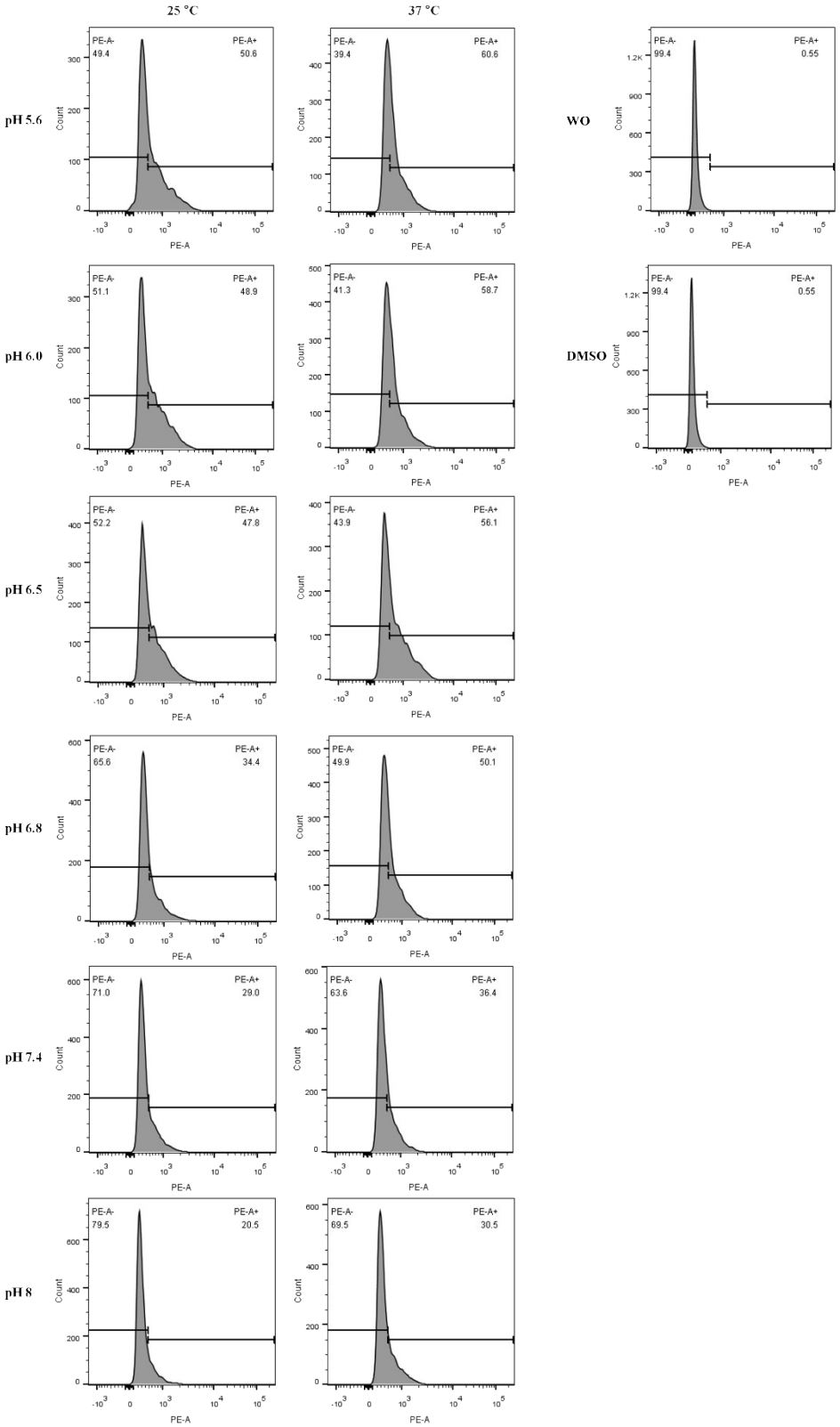

Fig. S8. Flow cytometric analysis of A2780 ovarian cancer cells after incubation with Dox-loaded p(NIPAM)$_{30}$-SS-*b*-p(Lys)$_{30}$-*b*-p(CL)$_{125}$ micelles under different pH and temperature conditions for 3 h.

Table S1. Comparison of tumor accumulation of p(NIPAM)$_{30}$-SS-*b*-p(Lys)$_{30}$-*b*-p(CL)$_{125}$ with various polymeric nanocarriers exhibiting high fluorescence intensity from non-tumor organs.

Entry	Nanocarrier	Targeting group	Preferred site of accumulation	Ref.[a]
1	CMP-Pp IX	CMP	liver	S1
2	PS-g-OEMPEG-DOX	No	liver	S2
3	T-S-NLC	TISWPPR	liver	S3
4	AIEgen-lipid conjugate	Lipid	liver	S4
5	MGC-GNP/PTX	MGC peptide	liver	S5
6	PDFDP	Anti-HER2	liver	S6
7	RGD-modified-lipid-calcium carbonate	RGD	liver/kidney	S7
8	Tf-QLPVM	Tf	liver/spleen	S8
9	DIR/His-SA-BSP	SA-BSP	liver	S9
10	cRGD-PTN-DOX	RGD	liver/kidney	S10
11	FA-PLGA-Pba	FA	liver/kidney	S11
12	Natura egg yolk lipid nanovector	FA	Liver/spleen	S12
13	p(NIPAM)$_{30}$-*b*-p(Lys)$_{30}$-*b*-p(CL)$_{125}$	No	tumor	this work

CMP-Pp IX : C_{16}-K(protoporphyrin IX)-GRRRR-AEEA-K(FAM)SDEVDSK(Dabcyl)-PEG$_8$-PEG$_8$; PS-g-OEMPEG-DOX : ortho ester-linked PEGylated poly(disulfide)-based micelle-doxorubicin; T-S-NLC = TISWPPR-PEG-modified salinomycin loaded nanostructured lipid carriers; AIEgen® : a fluorogen with aggregation-induced emission characteristics; MGC-GNP/PTX : M2 and C7 peptides decorated glutathione-sensitive nanoparticle/paclitaxel; PDFDP : click-functional PEG grafted amphiphilic polymer to coat hydrophobic AIE-active polymer; CMP : Cell membrane-targeted peptide; QLPVM : glutamine-leucine-proline-valine-methionine peptide; Tf : transferrin; DIR/His-SA-BSP : DIR labelled histidine-stearic acid-Bletilla striata polysaccharides;; cRGD-PTN-DOX : cyclic arginine-glycine-aspartic acid-PEG-poly(L-tyrosine); FA-PLGA-Pba : folate-poly(lactic-co-glycolic acid)-pheophorbide.

[a]References

S1. W. Ma, S. N. Sha, P. L. Chen, M. Yu, J. J. Chen, C. B. Huang, B. Yu, Y. Liu, L. H. Liu and Z. Q. Yu, *Adv. Healthc. Mater.*, 2019, **9**, e1901100.

S2. G. Yan, Y. Huang, D. Li, Y. Xu, J. Wang, X. Wang and R. Tang, *Eur. J. Pharm. Biopharm.*, 2019, **145**, 54–64.

S3. J. Zhou, M. Sun, S. Jin, L. Fan, W. Zhu, X. Sui, L. Cao, C. Yang and C. Han, *Drug Deliv.*, 2019, **26**, 281–289.

S4. X. Cai, D. Mao, C. Wang, D. Kong, X. Cheng and B. Liu, *Angew. Chem. Int. Ed. Eng.*, 2018, **57**, 16396–16400.

S5. T. Cui, X. Li, Y. Shu, X. Huang, Y. Wang and W. Zhang, *Int. J. Pharmaceut.*, 2018, **552**, 16–26.

S6. Y. Wu, Z. Chen, P. Zhang, L. Zhou, T. Jiang, H. Chen, P. Gong, D. S. Dimitrov, L. Cai and Q. Zhao, *Chem. Comm.*, 2018, **54**, 7314–7317.

S7. J. Q. Peng, S. Fumoto, T. Suga, H. Miyamoto, N. Kuroda, S. Kawakami and K. Nishida, *J. Control. Release*, 2019, **302**, 42–53.

S8. S. Lakkadwala, B. dos Santos Rodrigues, C. Sun and J. Singh, *Nanomed-Nanotechnol.*, 2020, **23**, 102112.

S9. C. Wang, J. Zhu, J. Ma, Y. Yang and X. Cui, *Int. J. Pharm.*, 2019, **567**, 118436.

S10. X. Gu, Y. Wei, Q. Fan, H. Sun, R. Cheng, Z. Zhong and C. Deng, *J. Control. Release*, 2019, **301**, 110–118.

S11. J. Son, S. M. Yang, G. Yi, Y. J. Roh, H. Park, J. M. Park, M.-G. Choi and H. Koo, *Biochem. Biophys. Res. Commun.*, 2018, **498**, 523–528.

S12. Z. Tang, C. Luo, Y. Jun, M. Yao, M. Zhang, K. He, L. Jin, J. Ma, S. Chen, S. Sun, M. Tao, L. Ding, X. Sun, X. Chen, L. Zhang, Y. Gao and Q.-l. Wang, *ACS appl. Mater. Interfaces*, 2020, **12**, 7984–7994.